



# Structural, Optical and Thermal Characterizations of PVA/MAA:EA Polyblend Films

Tellamekala Siddaiah<sup>a</sup>, Pravakar Ojha<sup>a</sup>, Neeruganti Obularajugari Gopal Velikanti Ramesh Kumar<sup>a</sup>,  
Chekuri Ramu<sup>a\*</sup> 

<sup>a</sup>Department of Physics, Vikrama Simhapuri University PG Centre, Kavali, 524201, India

Received: November 04, 2017; Revised: March 19, 2018; Accepted: June 05, 2018

Films of polyvinyl alcohol (PVA), Methacrylic Acid - Ethyl Acrylate (MAA:EA) copolymer and their blends PVA:MAA:EA of composition 80:20, 60:40, 50:50, 40:60, 20:80 (wt %) were prepared by using the solution cast technique. The prepared films were investigated by structural, optical and thermal studies. X-ray diffraction (XRD) scans revealed the semicrystalline nature of the blends for lower concentrations of PVA up to 60 wt % and the amorphous nature for higher ones. Fourier transform infra-red spectroscopy (FTIR) of blend samples indicates that there is a compatibility between PVA and MAA:EA copolymers through the formation of hydrogen-bonding between their polar groups. SEM image of polymer blend suggested the presence structural reorganization of polymer chains. UV-Visible spectral analysis revealed that the intensity of the shoulder around 271 nm decreases with increasing MAA:EA content. In DSC analysis, a single glass transition temperature for each blend was observed, which supports the existence of compatibility of such systems. From the observed results, 50:50 (wt %) PVA/MAA:EA is found to be the optimum blending ratio.

**Keywords:** PVA/MAA:EA film, XRD, FTIR, SEM, TGA, DSC, optical and thermal parameters.

## 1. Introduction

Polyvinyl alcohol (PVA) is a polymer with carbon chain backbone attached with hydroxyl groups. These OH groups can be a source of hydrogen bonding and hence assist in the formation of polymer blends. PVA is non-toxic, water-soluble synthetic polymer, which is widely used in the polymer blends due to its good physical and chemical properties, excellent film forming characteristics, emulsifying capability, non-carcinogenic, biodegradable and biocompatible qualities<sup>1</sup>. These unique characteristics enable it for its applicability in pharmaceutical fields, drug coating agents, material for surgical structures and cosmetic industries<sup>2</sup>.

Nowadays, the polymer electrolytes are of immense interest because of their potential applications in the field of thin film formation, interfacial contacts, desirable sizes etc. The development of miniature electronic gadgets like mobile phones and laptops has been remarkable in the last decade to a strong need for high energy batteries. However, those polymer electrolytes are unable to satisfy certain properties such as good mechanical strength, high ionic conductivity, long - term phase stability, tensile strength, and good abrasion resistance. In order to overcome these drawbacks, copolymers (or blending of polymers) have been considered for enhancing the properties of polymer electrolytes. Polymer blend can be more useful because of its easier preparation method and its ease to control the properties of polymer electrolytes by changing the composition of the blended polymer. These polymer blends have gained an ever - increasing importance as an excellent way to develop, without chemical synthesis, new materials with improved

properties. From the scientific point of view, polymer blends can enlighten structural properties relationships helping us to understand the underlying physics of polymer interactions. Due to the importance in the field of polymer applications, special emphasis has been given to those blends in which the polymeric components are believed to be mixed at the molecular level mixtures<sup>3</sup>.

Recently, some of the polymer blend electrolytes such as (PVA - PANI)<sup>4</sup>, (PVA - PAN), (PVP - PVA)<sup>5,6</sup>, (PMVEMA - PVA), (PVA - PEI), (PVA - PVdF), (PEO - PVA)<sup>7</sup>, (PVA - PAA)<sup>8</sup>, (PVA - PEG)<sup>9</sup>, (PEO - PMMA)<sup>10</sup>, (PVC - PS), (Chitosan - PVA)<sup>2</sup>, (PVA - NyC), (PEMA - PVdF), (PVA - NaAlg) etc. have been studied extensively by various techniques. These polymer electrolytes satisfy most of the properties required in the field of battery applications.

Methacrylic Acid - Ethyl Acrylate (MAA:EA) copolymer has been occupied the center stage amongst the copolymers because of its good environmental stability, easier processability and transparency. MAA:EA copolymer is having a substantial charge capacity and dopant dependent electrical and optical properties<sup>11</sup>. Both PVA and MAA:EA possesses film forming property. Accordingly, PVA/ MAA:EA film was thought to be a good candidate to enhance the cost to performance ratio on commercial products and of significant practical applications<sup>12</sup>.

However, polyvinyl alcohol (PVA) - Methacrylic Acid-Ethyl Acrylate (MAA:EA) polymer blend electrolyte has yet to be studied. In the present work, structural, optical and thermal properties of PVA/MAA:EA blends in the range of composition 80:20, 60:40, 50:50, 40:60, 20:80 wt% were investigated.

\*e-mail: [chramu8@gmail.com](mailto:chramu8@gmail.com)

## 2. Materials and Methods

MAA:EA copolymer (1:1) dispersion 30 percent is a dispersion in water of a copolymer of Methacrylic Acid and Ethyl Acrylate having a mean relative molecular mass of about 250000 (supplied by Merck Millipore India Ltd.) and had high purity. Polymer films of PVA/MAA:EA blend in different concentrations were prepared at room temperature by solution casting method. The desired concentrations of PVA/MAA:EA solution (80:20, 60:40, 50:50, 40:60, 20:80wt %) were prepared by using distilled water. The solution was stirred magnetically for 10-12 hours to get a homogeneous mixture and then cast onto plastic dishes. The solution was slowly evaporated at room temperature to obtain free-standing pure and blended films at the bottom of the dishes.

In order to investigate the nature of the copolymer films, differential scanning calorimetry (DSC) measurement was carried out by a SEIKO calorimeter (DSC - 220) with a continuous heat rate of 10°C/min under a nitrogen atmosphere from 40 to 600°C. The thermogravimetric analysis (TGA) was done using SEIKO thermal analysis system (TGA - 20) in the presence of nitrogen flow from 40 to 600°C, at the heating rate of 10°C/min. X-ray diffraction measurements were carried out using a Siemens D5000 diffractometer with CuK $\alpha$  radiation ( $\lambda = 1.5406 \text{ \AA}$ ). The films were scanned at  $2\theta$  angles between 10 and 40° with a step size of 0.02°. FTIR spectra of these films were recorded using a Perkin-Elmer FTIR spectrometer. The morphology of the polymer films was characterized by the Hitachi (TM - 3000 and H - 8100) electron microscope with scanning attachment. The spectra were taken over a wavenumber range 500 - 4000  $\text{cm}^{-1}$ . UV-Vis absorption spectra of the prepared samples were recorded in the range 200 - 800 nm at room temperature using JASCO UV-VIS-NIR spectrophotometer (model - V.700). From the optical absorption data, the optical constants such as band edge, optical band gap (both direct and indirect) were determined.

## 3. Results & Discussion

### 3.1. Fourier transform infra-red spectroscopy (FTIR)

Polymer structure and their chemical species could be investigated by using FTIR spectroscopy. Infrared spectra of these materials vary according to their composition and may be able to show the occurrence of complexation and interaction between various constituents. The mutual interaction between them generates change in their vibrational modes of the atoms or molecules in the material which introduces change in physical and chemical properties of the constituents of the complex.

The FTIR spectrum for pure MAA:EA copolymer is shown in the Figure 1. The spectrum exhibits bands characteristics

of stretching, bending vibrations of O - H, C - H, C = O, CH<sub>3</sub> - O and CH<sub>2</sub> +  $\alpha$  - CH<sub>3</sub> groups. The observed FTIR band positions and their assignments are presented in Table 1. In this film, a strong band observed at 1452  $\text{cm}^{-1}$  has been assigned to bending mode vibration corresponding to CH<sub>3</sub> group, while another strong band observed at 1492  $\text{cm}^{-1}$  has been attributed to C - H bending of CH<sub>2</sub><sup>13</sup>. The FTIR absorption bands appeared as weak bands in 1601  $\text{cm}^{-1}$  range are attributed to carbonyl stretching of the acid and ester units<sup>14</sup>. A broad and very strong band observed at 2923  $\text{cm}^{-1}$ , arising from C - H stretching frequency shows the presence of methylene group<sup>11</sup>. Asymmetric C - H stretching of methyl groups shows a peak at 3026  $\text{cm}^{-1}$  and C - H stretching of the methylene group gives two peaks at 3059  $\text{cm}^{-1}$  and 3082  $\text{cm}^{-1}$ .

As shown in Figure 2, the FTIR spectrum of pure PVA exhibits several bands characteristic of stretching and bending vibrations of O - H, C - H, C = C and C - O groups. A broad and very strong band observed at 2813 - 3601  $\text{cm}^{-1}$ , which arises from O - H stretching frequency is an indicator of the presence of hydroxyl groups. Another band observed at 2905  $\text{cm}^{-1}$  indicates an asymmetric stretching mode of the CH<sub>2</sub> group. The band corresponding to CH<sub>2</sub> symmetric stretching vibration occurs at about 2168  $\text{cm}^{-1}$ . Absorbance at 1720  $\text{cm}^{-1}$  corresponds to an acetyl C = O group, which could be explained on the basis of intermolecular hydrogen bonding with the adjacent OH group. The shape of the carbonyl bands (C = O) for blend samples is different from that of pure

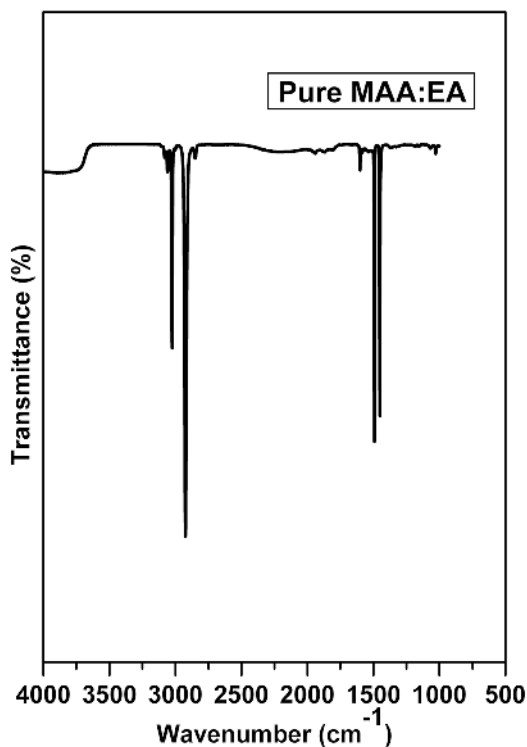


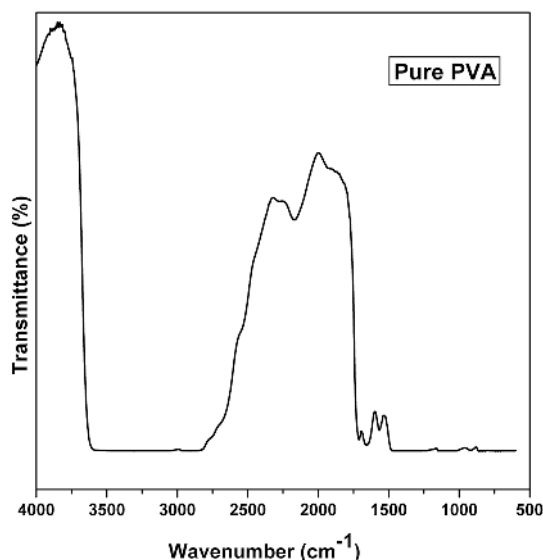
Figure 1. FTIR spectrum of pure MAA:EA copolymer

**Table 1.** FTIR peak assignment of pure and PVA/MAA:EA blend films.

Wavenumber (cm <sup>-1</sup> )	Band assignment
1452	CH <sub>3</sub> -O bending
1492	C-H bending of CH <sub>2</sub>
1601	C=O stretching
2923	C-H stretching of methylene group
3026	C-H stretching methyl group
3059	C-H stretching methylene group
3082	C-H stretching methylene group
2813 - 3601	O-H stretching frequency
2905	Asymmetric stretching mode of CH <sub>2</sub> group
2168	CH <sub>2</sub> symmetric stretching vibration
1711	C=O stretching
1658	C=C stretching
1566	C=C stretching vibration
1349	CH + OH combination frequencies
1080	C-O stretching
918	C-C stretching

homopolymers, indicating a change in the balance of true and associated carbonyl groups in the blends. The increase in the multiplicity of hydroxyl band (OH) with increasing MAA:EA content in the blend samples may reflect possible interactions through hydrogen bonding of hydroxyl bread on the backbone of PVA and MAA:EA. Similar behavior was observed by Attia and Abd El - Kader<sup>12</sup> on PVA/ 2HEC polyblend films. The increased intensity of bands indicates that greater amount of MAA:EA have complexed with the oxygen and hydrogen atoms. The effect of blending on the modes of vibration is observed interms of increase in the intensity of bands and appearance of new bands, which results from the formation of crosslinks between the MAA:EA and oxygen atoms of carbonyl groups. This indicates the increase in the basicity of C = O groups with an increase in the MAA:EA concentration. Absorption band observed at 1711cm<sup>-1</sup> is due to C = O of carbonyl group. A moderate absorption peak at 1658 cm<sup>-1</sup> has been attributed to the C = C stretching mode. Another band at 1566 cm<sup>-1</sup> was attributed to stretching vibration of C = C and a characteristic alcohol band at 1080 cm<sup>-1</sup> was assigned to the stretching of C - O of PVA, which is affected by hydrogen bonding along with C - H and O - H bending<sup>15</sup>. A C - C stretching mode of absorption is observed at 918 cm<sup>-1</sup>. The band observed at 1349 cm<sup>-1</sup> has been attributed to combination frequencies of (CH + OH).

The miscibility between the polymer and the copolymer (PVA / MAA:EA) blend is due to the hydrogen bonding between PVA hydroxyl groups and carbonyl groups of MAA:EA copolymer. The possibility of interactions between the polymer pair in the blend through specific polar groups is examined using FTIR analysis. FTIR spectra of PVA/

**Figure 2.** FTIR spectrum of pure PVA

MAA:EA blends (80:20, 60:40, 50:50, 40:60, 20:80 wt %) are also shown in Figure 3(a - e). The FTIR spectra of all blended films exhibit bands, whose vibrational frequencies are found to be similar to several bands observed for pure PVA polymer film. IR features of PVA are more dominant even in 20:80 composition because PVA sample has dense molecular packing in the crystal and also stronger intermolecular hydrogen bonds comparing with MAA:EA, which are responsible for disappearance of functional groups of MAA:EA in the polymer blend. The FTIR spectrum shows shift in some of the band positions and change in the intensities of some other bands compared with pure films. O - H stretching frequency observed at 2813 - 3601 cm<sup>-1</sup> for pure PVA shows a large shift towards the low-frequency region in the blended films, which indicates the presence of a broad range of associated hydroxyls in blended films. The CH<sub>2</sub> stretching frequency at 2905 cm<sup>-1</sup> shifts towards higher frequency for all the blends and the shift is found to be very high for 50:50 (wt %) blend i.e 2939cm<sup>-1</sup>. CH<sub>2</sub> stretching frequency observed at 2905cm<sup>-1</sup> for pure PVA disappeared for 40:60 (Wt %) blend film. This change indicates the possibility of MAA:EA copolymer to be attached to methylene (CH<sub>2</sub>) and C - H in the side chain of PVA molecule<sup>16</sup>. The shift in the 2813 - 3601 cm<sup>-1</sup> band corresponding to OH groups resulted from in inter/intramolecular interactions in PVA/MAA:EA blends. The band at 2168 cm<sup>-1</sup> is assigned to CH<sub>2</sub> symmetric stretching vibrations. For the blend samples, the band shifts to lower frequency and the intensity of the band is decreased, which indicates the change in the chemical structure.

The appearance of a band at 1658 cm<sup>-1</sup> (C = C) confirms the semi-crystalline nature of the blends as reported by Ragab<sup>6</sup>. A weak peak around 1658 cm<sup>-1</sup> is observed in the present work, which confirms the semicrystalline nature

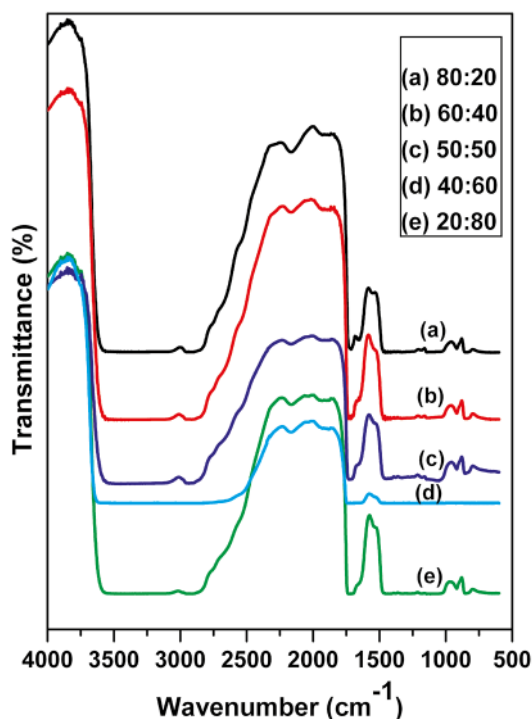


**Figure 3.** FTIR curves of PVA/MAA:EA blend samples (a) 80:20 (b) 60:40 (c) 50:50 (d) 40:60 (e) 20:80

polymer blend films. This occurs as the elimination of water proceeds isolating C = C in acyclic ring structure.

The small absorption band around  $918\text{ cm}^{-1}$  was found to be characteristic of the syndiotactic structure of the prepared films, Nagura et al.<sup>17</sup> reported that the syndiotacticity of the PVA samples causes dense molecular parking in the crystal and stronger intermolecular hydrogen bonds, which in turn are responsible for the disappearance of the molecular motion. This band was appeared in the spectra of pure PVA and other blend samples. These results manifested the conclusion of the specific interaction in PVA/MAA:EA blend matrix. In the case of PVA/MAA:EA, FTIR spectra shows shifts in some bands and change in the intensities of other bands comparing with the pure films which indicates the considerable coupling between the polymer and copolymer.

### 3.2. Differential scanning calorimetry (DSC)

Thermal characterization techniques are the convenient tools to determine the physical and chemical changes such as phase transitions, glass transition temperature ( $T_g$ ) and melting temperature ( $T_m$ ). A temperature range of  $0 - 250^\circ\text{C}$  at a heating rate of  $10^\circ\text{C}/\text{min}$  was utilized under nitrogen atmosphere. The DSC patterns in Figure (4) show endothermic peaks of glass transition temperature ( $T_g$ ) and melting temperature ( $T_m$ ).  $T_g$  of polymer blends is a typical characteristic which is used in studying the miscibility and interaction between polymers and  $T_m$  is mostly used in

investigating the crystallization of polymers. In Figure 4, one can see that all blended films have only one  $T_g$  indicating that the blends are homogeneous. Theoretically, the glass transition temperature of miscible polymer blends could be calculated by using Fox equation<sup>18</sup>.

$$\frac{1}{T_{g(\text{blend})}} = \frac{W_1}{T_{g_1}} + \frac{W_2}{T_{g_2}} \quad (1)$$

In which  $W_1, W_2$  and are weight fractions and the glass transition temperatures of component 1 and 2 respectively. The observed transition temperature  $T_{g(\text{o})}$  and theoretical value  $T_{g(\text{th})}$  of the blends are presented in Table 2.

For pure PVA,  $T_g$  observed is  $96.3^\circ\text{C}$ <sup>19</sup> and for copolymer (MAA:EA) shown in the Figure 5, it is  $103^\circ\text{C}$ <sup>11</sup>. The small traces at about  $41^\circ\text{C}$  for the MAA:EA sample could be due to a small amount of moisture. The  $T_g$  for blend varies from 90 to  $103.6^\circ\text{C}$  with the blend ratio. All the observed transition temperatures show variation compared to their theoretical values calculated by equation (1). This deviation from the theoretical value of the glass transition temperature is also observed in an earlier report<sup>20</sup> in which they attributed this behavior to deviation with respect to free volume linearity in the blends. Changes in the free volume are related to specific interactions between polymer chains, increasing specific interactions lead to the formation of a more compact molecular network and diminish the free volume of molar

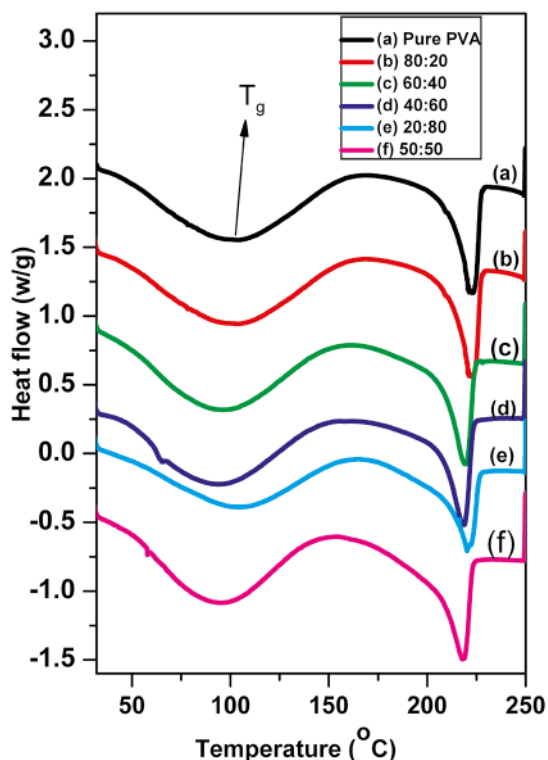


**Figure 4.** DSC curves of (a) Pure PVA and PVA/MAA:EA blend sample (b) 80:20 (c) 60:40 (d) 40:60 (e) 20:80 (f) 50:50

**Table 2.** Comparison of observed transition temperatures  $T_{g(o)}$  and theoretical Value  $T_{g(th)}$  of the blends.

PVA/MAA:EA	$T_{g(th)}$ °C	$T_{g(o)}$ °C
20:80	100.00	103.6
40:60	99.07	94.7
60:40	98.3	95.0
80:20	97.21	99.6
50:50	98.59	90.0

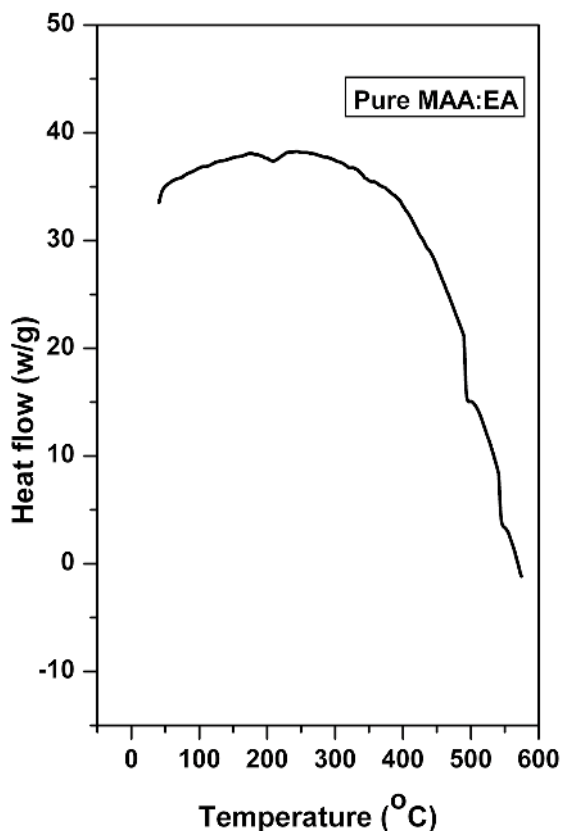
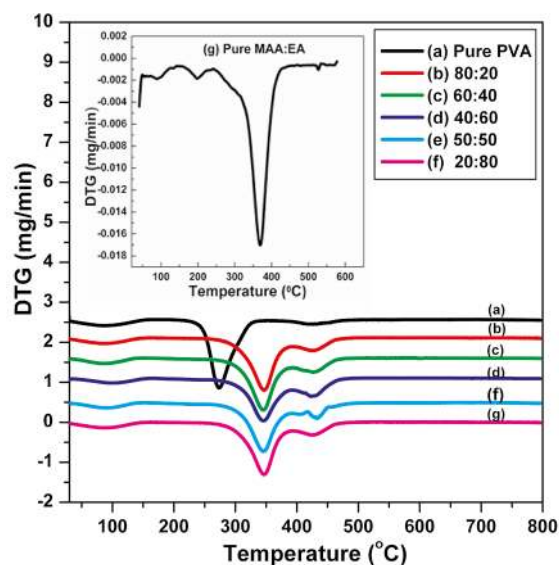
chains. In this system, the mobility of the chains decreases due to the presence of hydrogen bonds.

An endothermic peak was observed at around 222°C for pure PVA and MAA:EA copolymer shows it at 210°C, which corresponds to the melting temperature of PVA and MAA:EA respectively. A slight shift of  $T_m$  towards lower temperature has been observed for blended samples, which reveals the transition from semi-crystalline to an amorphous phase. The lowering of  $T_m$  for blend films is quite common and has been related to decreasing spherulite sizes<sup>21</sup> and their surface free energy. As a result of more flexible amorphous environment getting trapped in or adjacent to the crystalline matrix, the suppressed crystalline portion of the MAA:EA copolymer melts probably at lower temperatures. This clearly indicates the suppression of crystallites and there by increase in the amorphous content in the polymer. This leads to favoring in transport and thus to enhance the ionic conductivity of the electrolyte<sup>22</sup>.

### 3.3. Thermogravimetric analysis (TGA)

Figure (6), shows dTG thermograms of pure films and PVA/MAA:EA blends with a heating rate of 10°C/min in the temperature ranging from room temperature to 800°C. It is found that there are three temperature regions over which most of the weight loss occurs. These stages can be distinguished in the diagram of weight loss (TG%) during heating as well as more clearly in the diagram of derivative mass loss (DTA). The decomposition steps and percentage weight loss for individual polymers and their blends are represented in Table 3.

For pure PVA the first weight loss occurs between 30 - 157°C with a weight loss of 13 %, which corresponds to the removal of water. The second weight loss occurs between 219 - 345°C and corresponds to the thermal degradation of PVA intermolecular hydrogen bonding. The third degradation between 387 - 479°C corresponds to the decomposition of PVA main backbone chain. The DTG curve of the pure MAA:EA copolymers shown in inset of Figure (6), reveals that there are three distinct steps of weight loss. The 4 - 5% weight loss below 170°C is attributed to the loss of adsorbed water<sup>23</sup>. The second and third steps observed in the temperature ranges 210 - 400°C and above 400°C are the regions of major weight loss and appeared to be due to the extensive degradation of the polymer backbone. The

**Figure 5.** DSC curve of pure MAA:EA copolymer**Figure 6.** DTG curves of pure and blended PVA/MAA:EA samples (a) Pure PVA (b) 80:20 (c) 60:40 (d) 40:60 (e) 50:50 (f) 20:80 (g) Pure MAA:EA

second decomposition occurred at 210°C is attributed to the elimination of evaporated molecules in the side groups of MAA:EA copolymer and the third decomposition at above 400°C is due to quantized graft chain degradation<sup>24</sup>.



**Table 3.** TGA and DTG data for individual Polymers and their blends of PVA/ MAA:EA (wt/wt).

PVA/ MAA:EA (wt/wt)	Temperature (°C)			Weight loss (%)	
	Start	End	T <sub>p</sub>	Partial	Total
Pure PVA	30	157	95	13	83
	219	345	273	73	
	387	479	425	7	
80:20	32	147	87	11	92
	261	387	346	63	
	388	472	427	18	
60:40	30	132	87	9	92
	273	385	347	64	
	386	475	427	19	
40:60	35	147	106	9	89
	271	387	346	59	
	388	477	426	21	
20:80	28	142	86	12	87
	247	390	346	60	
	395	465	426	15	
50:50	25	139	92	9	90
	264	410	345	64	
	411	465	431	17	
Pure MAA:EA	46	135	86	7.5	87
	135	243	194	35	
	243	458	367	55.65	

The blends of PVA and MAA:EA also exhibit three weight loss stages as shown in Figure (6), followed by a final decomposition at 500°C for all the membranes. The lower values of weight loss percentage in the first decomposition step are responsible for the volatilization of small molecules and or evaporation of residual absorbed water. The second weight loss may be due to the splitting of monomers and bond scission in the polymeric backbone and also the ionic interaction between the homopolymers. The major weight loss percentage in the third decomposition step is attributed to fragmentation of the macromolecular structure of both PVA polymer and MAA:EA copolymer<sup>12</sup>. The blends thus exhibit a relatively good thermal stability than pure films. Therefore, it can be concluded that the blend sample of 50:50 wt % has a more thermal stability and lower order than the other samples.

### 3.4. X - ray diffraction analysis (XRD)

The X-ray diffraction technique is a useful tool to determine the structure and crystallization of the polymer

matrices. Figure 7 shows the X - ray diffraction patterns of PVA and MAA:EA copolymers as well as their blend samples at room temperature in the scanning range  $0^\circ \leq 2\theta \leq 40^\circ$ . Pure PVA spectrum [Figure 7 (a)] shows small peaks at  $2\theta = 0.6^\circ$ ,  $1.46^\circ$  and relatively broad peak at  $2\theta = 19.52^\circ$  diffused in the hallow amorphous region<sup>25</sup>. The appearance of sharp reflections and diffuse scattering is characteristic of crystalline and amorphous phases of convectional semicrystalline polymers. Accordingly, the PVA/MAA:EA blends [Figure 7 (b-f)] also exhibited semicrystalline nature. From the spectra of PVA/MAA:EA blends, one distinct peak at  $2\theta = 19.52^\circ$  corresponding to crystal, which is responsible for separation as it comprises of functional groups such as  $-\text{CH}_2 - \text{CH}_3$  and  $-\text{OH}$ , has not undergone any significant change after adding more amount of PVA. However, the spectrum of pure MAA:EA copolymer shown in the inset of Figure 7 exhibits a broad amorphous halo with a scattered intensity maximum corresponding to  $2\theta = 16.39^\circ$ . The patterns revealed that there are no sharp diffraction lines and the broad background scattering of MAA:EA copolymer suggests the presence of amorphous nature.

XRD patterns of blend samples with concentrations 60, 40, 20 and 50 (wt %) PVA (Figure 7) exhibit the characteristics of pure PVA, but varying intensity for the reflection peak.

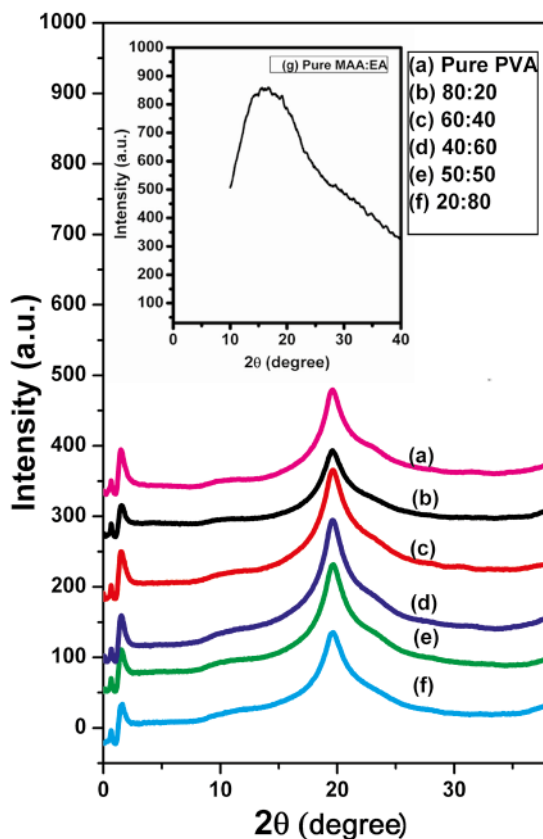


**Figure 7.** XRD curves of pure and blended PVA/MAA:EA samples (a) Pure PVA (b) 80:20 (c) 60:40 (d) 40:60 (e) 50:50 (f) 20:80 (g) Pure MAA:EA

Thus, one can say that the semicrystalline nature of PVA is decreased upon mixing with the relatively higher content of MAA:EA copolymer. For such blends, compatibility between the semicrystalline and amorphous components of copolymers is possible. Thus, it can be suggested that the crystalline forms in PVA do not prevent the compatibility between amorphous regions of the two polymers in the blend system<sup>26</sup>. The tendency of varying crystallinity in blend sample implies a decrease of a number of hydrogen bonds that are formed between PVA and MAA:EA if present<sup>7</sup>.

It can be seen that the peaks at  $\theta = 0.6^\circ$  and  $1.46^\circ$  got slightly displaced in the complex 80 wt % PVA polymer blend film. The intensity of the peak at  $2\theta = 19.52^\circ$  decreased and peak width increased to 80 wt % of PVA film. The decrease in the intensities of 80 % complexed PVA blend films causes a decrease in the degree of crystallinity and a simultaneous increase in the amorphous nature of complexed films. Hence this amorphous nature of the film is responsible for greater ionic diffusivity which may results in high ionic conductivity, which can be obtained in amorphous polymers that have flexible backbone<sup>16</sup>. This observation confirms that complexation has taken place in the amorphous phase.

### 3.5. Scanning electron microscopy (SEM) Studies

The Scanning electron microscope produces images of a sample by scanning it with a focused electron beam. The beam of electrons interacts with electrons in the sample, which produces various signals that can be detected and that contain the information about the sample's surface morphology and composition. The beam of electrons generally scanned by the method of raster scan pattern, and the position of the beam is combined with detected signal to create an image.

SEM is often used to study the compatibility between various components of the polymer electrolytes through the detection of phase separations and interfaces<sup>27,14</sup>. The compatibility between the polymer blend and the inorganic dopants has great influence on the properties of thermal, mechanical and ionic conductivity of the polymer electrolytes.

Figure 8 (a-c) shows the SEM images of Pure MAA:EA, Pure PVA and PVA/MAA:EA (50:50) blend. It can be seen from Figure 8 (a) that pure MAA:EA copolymer film shows smooth surface, suggesting that MAA and EA molecules may disperse in the soft-segment phase with little influence on the micro phase separation and mixing of the hard and soft segments<sup>28</sup>. SEM of pure PVA film exhibits no features attributable to any crystalline morphology as shown in Figure 8 (b). So the semicrystallinity of PVA discussed earlier is likely to be submicroscopic in nature. SEM image of polymer blend electrolyte is shown in Figure 8 (c). The side branches are not well correlated along the length of the dendrites trunk. The growth of the dendritic-like shape, which represents the gathering of the branched aggregate clusters, became more clear leading to the formation of condensed

aggregated dendrites shape. This suggests the presence of structural reorganizations of polymer chains<sup>10</sup>.

### 3.6. UV - Visible absorption studies

The study of optical absorption, the absorption edge, in particular, has been proved to be the very useful in the elucidation of the optical properties and optical constants of crystalline and non - crystalline materials. Figure 9 shows the absorption spectra of PVA and MAA:EA copolymers and their blends 80:20, 60:40, 50:50, 40:60, and 20:80 (wt %) PVA/MAA:EA in the wavelength range 200 - 800 nm. The spectra of pure PVA and pure MAA:EA copolymer exhibited a shoulder like band at 274 and 221 nm as shown in Figure 9 (a) and insert of Figure 9 respectively, which may be due to  $\pi \rightarrow \pi^*$  electronic transition (k - band) of carbonyl groups<sup>29</sup>. All the blended samples contain only one remarkable shoulder like a band with an irregular deviation in the position. The absorption of all blended samples increases as copolymer content increases. This is the evidence for the miscibility between copolymers. The UV - Visible spectra for the blended PVA/MAA:EA samples with the composition of 40:60, 50:50, and 20:80 (wt %) contained sharp intense bands at 213, 208 and 201 nm, beside a shoulder like band at about 276 nm.

The absorption coefficient ' $\alpha$ ' is related to absorbance ' $A$ ' by the equation

$$\alpha = 2.303 \times \left( \frac{A}{d} \right) \quad (2)$$

Where A is the absorbance and d is the thickness of the sample. When direct band gap exists, the absorption coefficient has the following dependence on the energy of the incident photon<sup>30</sup>

$$\alpha h\nu = C(h\nu - E_g)^{1/2} \quad (3)$$

Where  $E_g$  is the band gap, C is a constant,  $\nu$  is the frequency of light and h is plank's constant. A plot of  $(\alpha h\nu)^2$  vs  $h\nu$  is shown in Figure 10. The intercept on the energy axis on extrapolating the linear portion of the curve to zero absorption value may be taken as the value of the band gap. For both pure PVA and MAA:EA films, the direct band gap lies at 5.87 and 5.16 eV respectively. The direct band gap values for blended films vary from 5.77 eV to 5.05 eV and are presented in Table 4. For indirect transitions, which requires phonon assistance, the absorption coefficient has the following dependence on the photon energy<sup>11</sup>.

$$\alpha h\nu = A(h\nu - E_g + E_p)^2 + B(h\nu - E_g - E_p) \quad (4)$$

Where  $E_p$  is the phonon energy associated with transition and A and B are the constants depending on the band structure.

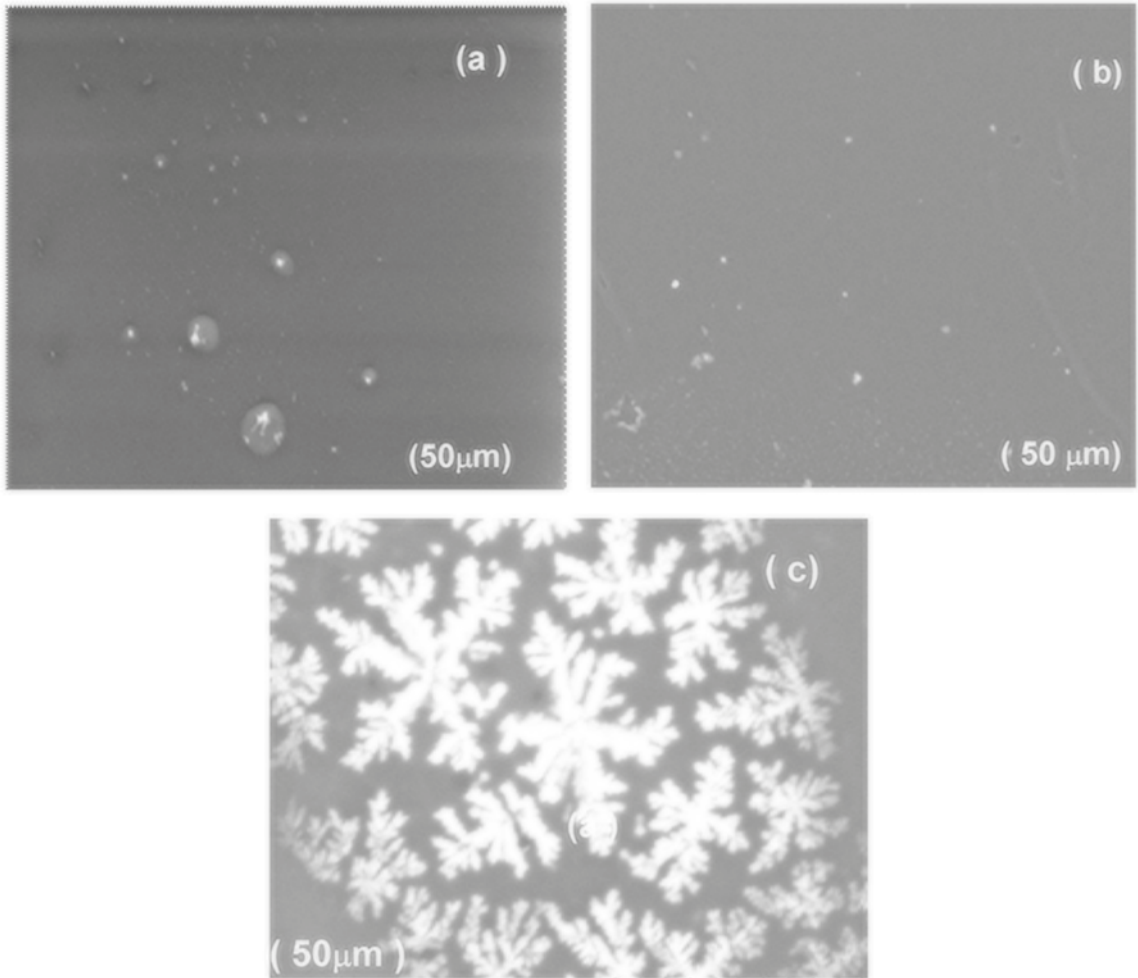


**Figure 8.** SEM images of (a) Pure MAA:EA (b) Pure PVA (c) PVA/MAA:EA (50:50) blend

The indirect band gap values can be calculated by plotting  $(\alpha h\nu)^{1/2}$  vs  $(h\nu)$  as shown in Figure 11. For both pure PVA and MAA:EA films, the indirect band gap values lie at 5.68 and 4.82 eV respectively. The values of all blended samples vary from 5.28 to 4.39 eV (Table 4).

The position of absorption edge was obtained by extrapolating the linear portion of  $\alpha$  vs  $h\nu$  plot (Figure 12) to zero absorption value. For both PVA and MAA:EA films, the absorption edge lies at 5.94 and 5.04 eV respectively, and the absorption edge for the blends vary from 5.79 to 4.83 eV (Table 4)

From Table 4, it is evident that the values of direct and indirect band gap varies with increase in MAA:EA content. This may be reflecting the induced changes in the number of available final states according to blend compositions<sup>12</sup>. Among the all blend samples, the sample with 50:50 (wt %) shows minimum optical band gap value (Table 4), this indicates that it shows more semiconducting nature than remaining blend samples.

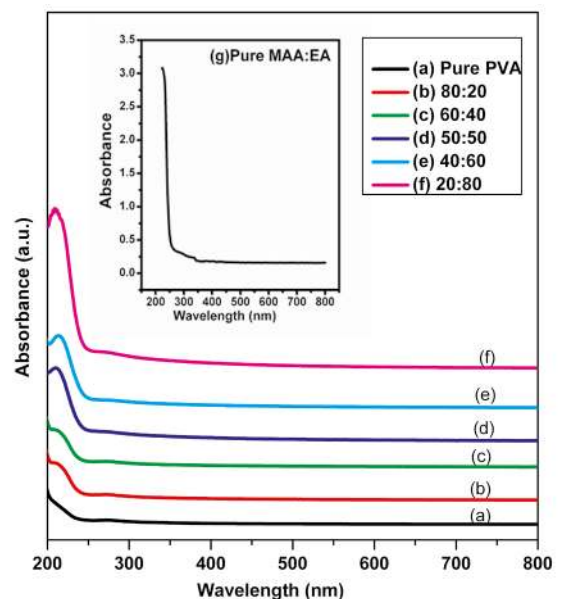


**Figure 9.** Absorption spectra of pure and blended PVA/MAA:EA samples (a) Pure PVA (b) 80:20 (c) 60:40 (d) 50:50 (e) 40:60 (f) 20:80 (g) Pure MAA:EA



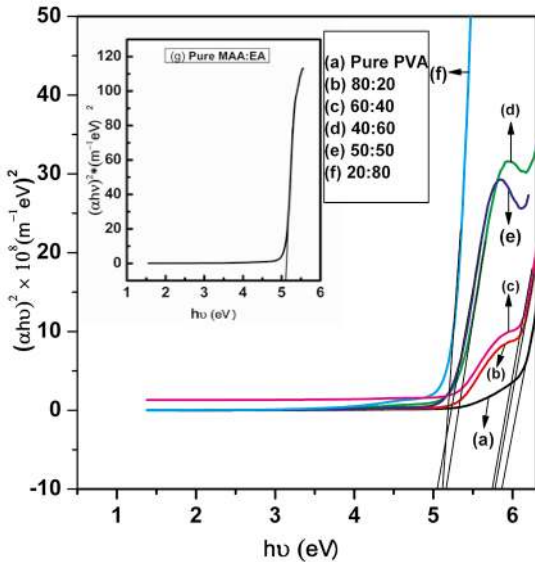


**Figure 10.**  $(\alpha h\nu)^2$  vs  $h\nu$  curves of pure and PVA/MAA:EA blend samples (a) Pure PVA (b) 80:20 (c) 60:40 (d) 40:60 (e) 50:50 (f) 20:80 (g) Pure MAA:EA

**Table 4.** Values of absorption edge and optical band gap of pure and PVA/MAA:EA blend samples.

PVA/ MAA:EA (wt/wt)	Absorption edge (eV)	Optical bandgap energy (eV)	
		Direct	Indirect
Pure PVA	5.94	5.87	5.68
80:20	5.79	5.77	5.28
60:40	5.62	5.74	5.21
50:50	4.83	5.05	4.39
40:60	4.89	5.16	4.47
20:80	5.04	5.12	4.68
Pure MAA:EA	5.04	5.16	4.82

## 4. Conclusions

The existence of maximum absorbing edge and minimum in band tail for 50:50 (wt/wt) % PVA/MAA:EA blend sample indicate that it has more carrier concentration in the localized levels. On the basis of the observed data from the XRD, FTIR, DSC and TGA, it could be concluded that the formation of hydrogen bonding between PVA and MAA:EA is possible within the investigated composition ranges. FTIR spectra of all blend samples shows the variation in the intensities of peaks with increasing the MAA:EA content in the polymer matrix, which indicate the considerable interaction between PVA and MAA:EA. XRD studies on the blend samples of 20, 40, 50 and 60 wt % PVA content revealed that the semi-crystalline structure of PVA is essentially sustained while

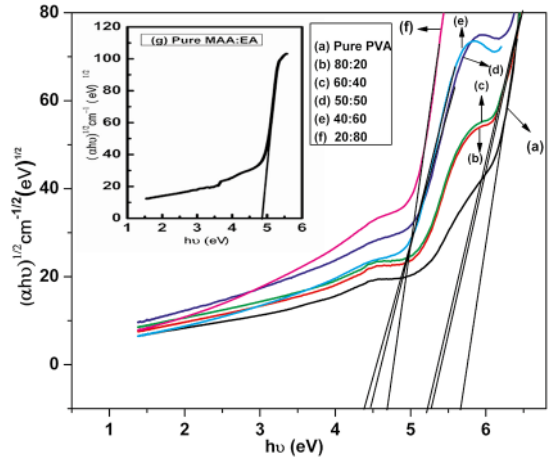


**Figure 11.**  $(\alpha h\nu)^{1/2}$  vs  $h\nu$  curves of pure and PVA/MAA:EA blend samples (a) Pure PVA (b) 80:20 (c) 60:40 (d) 50:50 (e) 40:60 (f) 20:80 (g) Pure MAA:EA

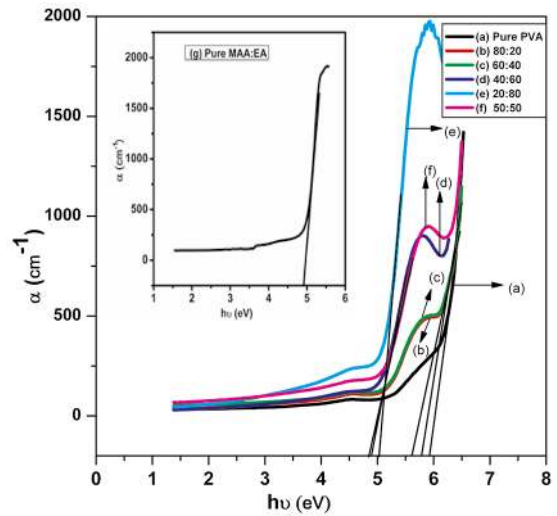


**Figure 12.**  $\alpha$  vs  $h\nu$  curves of pure and PVA/MAA:EA samples (a) Pure PVA (b) 80:20 (c) 60:40 (d) 40:60 (e) 20:80 (f) 50:50 (g) Pure MAA:EA

for relatively higher concentration 80 wt % the amorphous nature is observed. SEM image of polymer blend shows the dendrites like shape. Thermogravimetric analysis of pure and blend samples shows three distinct steps of weight loss, the first step corresponds to removal of water, second step is due to thermal degradation of intermolecular hydrogen bonding and the third step leads to decomposition of the main backbone chain. Out of all the blend samples, the blend with 50:50 (wt/wt) % PVA/MAA:EA shows higher decomposition temperature ( $T_d$ ). DSC analysis shows a single glass transition temperature for each blend, which supports the miscibility of the system and among the all blend samples, 50:50 (wt/wt) % PVA/MAA:EA sample shown lower melting temperature

(Tm). Out of all the blend films, PVA/MAA:EA with 50:50 (wt %) shows optimal properties.

## 5. References

1. Swaroop K, Francis S, Somashekarappa HM. Gamma irradiation synthesis of Ag/PVA hydrogels and its antibacterial activity. *Materials today: Proceedings*. 2016;3(6):1792-1798.
2. Abraham A, Soloman PA, Rejini VO. Preparation of Chitosan-Polyvinyl Alcohol Blends and Studies on Thermal and Mechanical Properties. *Procedia Technology*. 2016;24:741-748.
3. Muthuvinayagam M, Gopinathan C. Characterization of proton conducting polymer blend electrolytes based on PVdF-PVA. *Polymer*. 2015;68:122-130.
4. El-Sayed S, Abdel-Baset T, Elfadl AA, Hassen A. Effect of nanosilica on optical, electric modulus and AC conductivity of polyvinyl alcohol/polyaniline films. *Physica B: Condensed Matter*. 2015;464:17-27.
5. Shanthi B, Muruganand S. Structural, vibrational, thermal, and electrical properties of PVA/PVP biodegradable polymer. *International Journal of Scientific Engineering and Applied Science*. 2015;1(8):348-351.
6. Ragab HM. Spectroscopic investigations and electrical properties of PVA/PVP blend filled with different concentrations of nickel chloride. *Physica B: Condensed Matter*. 2011;406(20):3759-3767.
7. Abdelghany AM, Meikhaail MS, Elsheshtawy NA, Salah HY. Structural and Thermal Stabilization Correlation of PEO/PVA-AgCl Polymer Composites. *Middle East Journal of Applied Sciences*. 2015;5(5):1-6.
8. Abbas AK, Naife RM, Rashid FL, Hashim A. Optical properties of (PVA-PAA-Ag) nanocomposites. *International Journal of Science and Research*. 2015;4(1):2489-2492.
9. Rubee BH, AlHussien SA. Study of optical properties of (PVA-PEG-ZNO) nanocomposites. *International Journal of Science and Research*. 2016;5(5):1794-1799.
10. Okerberg BC, Marand H, Douglas JF. Dendritic crystallization in thin films of PEO/PMMA blends: A comparison to crystallization in small molecule liquids. *Polymer*. 2008;49(2):579-587.
11. Kumar YM, Bhyagyasree K, Gopal NO, Ramu C, Nagabhushana H. Structural, Thermal and Optical Properties of Mn<sub>2+</sub> Doped Methacrylic Acid - Ethyl Acrylate (MAA:EA) Copolymer Films. *Zeitschrift für Physikalische Chemie*. 2016;231(5):1039-1055.
12. Attia G, El-kaderA MFH. Structural, Optical and Thermal Characterization of PVA/2HEC Polyblend Films. *International Journal of Electrochemical Science*. 2013;8(4):5672-5687.
13. Kumar KK, Ravi M, Pavani Y, Bhavani S, Sharma AK, NarasimhaRao VVR. Investigations on PEO/PVP/NaBr complexed polymer blend electrolytes for electrochemical cell applications. *Journal of Membrane Science*. 2014;454:200-211.
14. Abdelrazek EM, Abdelghany AM, Oraby AH, Asnag GM. Investigation of Mixed Filler Effect on Optical and Structural Properties of PEMA Films. *International Journal of Engineering & Technology*. 2012;12(4):98-102.
15. Hemantha Kumar GN, Lakshmana Rao J, Gopal NO, Narasimhulu KV, Chakradhar RPS, VaradaRajulu A. Spectroscopic investigations of Mn<sup>2+</sup> ions doped poly(vinyl)alcohol films. *Polymer*. 2004;45(16):5407-5415.
16. Balaji Bhargav P, Madhu Mohan V, Sharma AK, Rao VVRN. Structural, Electrical and Optical Characterization of Pure and Doped Poly (Vinyl Alcohol) (PVA) Polymer Electrolyte Films. *International Journal of Polymeric Materials*. 2007;56(6):579-591.
17. Nagura M, Mastuzawa S, Yamaura K, Ishikawa H. Tacticity Dependence of Molecular Motion in Crystal of Poly(vinyl alcohol). *Polymer Journal*. 1982;14:69-72.
18. Larrañaga M, Mondragon I, Riccardi CC. Miscibility and mechanical properties of an amine-cured epoxy resin blended with poly(ethylene oxide). *Polymer International*. 2007;56(3):426-433.
19. Chen N, Zhang J. The role of hydrogen-bonding interaction in poly(vinyl alcohol)/poly(acrylic acid) blending solutions and their films. *Chinese Journal of Polymer Science*. 2010;28(6):903-911.
20. Mano V, Ribeiro e Silva MES, Silva ME, Barbani N, Giusti P. Binary blends based on poly(N-isopropylacrylamide): Miscibility studies with PVA, PVP, and PAA. *Journal of Applied Polymer Science*. 2004;92(2):743-748.
21. Bandara LRAK, Dissanayake MAK, Mellander BE. Ionic conductivity of Plasticized(PEO)-LiCF<sub>3</sub>SO<sub>3</sub> electrolytes. *Electrochimica Acta*. 1998;43(10-11):1447-1451.
22. Mohan VM, Qiu W, Shen J, Chen W. Electrical properties of poly(vinyl alcohol) (PVA) based on LiFePO<sub>4</sub> complex polymer electrolyte films. *Journal of Polymer Research*. 2010;17(1):143.
23. Farces S. Influence of gamma-ray irradiation on optical and thermal degradation of poly (ethyl-methacrylate) (PEMA) polymer. *Natural Science*. 2012;4(7):499-507.
24. Zain NF, Zainal N, Mohamed NS. The influences of ionic liquid to the properties of poly(ethylmethacrylate) based electrolyte. *Physica Scripta*. 2015;90(1):015702.
25. Liu C, Xiao C, Liang H. Properties and structure of PVP-lignin "blend films". *Journal of Applied Polymer Science*. 2005;95(6):1405-1411.
26. Cheung YW, Guest MJ. A study of the blending of ethylene-styrene copolymers differing in the copolymer styrene content: Miscibility considerations. *Journal of Polymer Science Part B: Polymer Physics*. 2000;38(23):2976-2987.
27. Zhang S, Lee JY, Hong L. Visualization of particle distribution in composite polymer electrolyte systems. *Journal of Power Sources*. 2004;126(1-2):125-133.
28. Madhav Kumar Y, Gopal NO, Ramu C, Babu S, Lakshmana Rao J, Nagabhushana H, et al. Structural, thermal and optical properties of Cu<sup>2+</sup> doped methacrylic acid-ethylacrylate (MAA:EA) copolymer films. *Bulletin of Materials Science*. 2017;40(5):877-886.
29. Shehap AM. Thermal and Spectroscopic Studies of Polyvinyl Alcohol/Sodium Carboxy Methyl Cellulose Blends. *Egypt Journal of Solids*. 2008;3(1):75-91.
30. Urbach F. The Long-Wavelength Edge of Photographic Sensitivity and of the Electronic Absorption of Solids. *Physical Review*. 1953;92(5):1324-1324.